Relationship between the Broad OH Stretching Band of Methanol and Hydrogen-Bonding Patterns in the Liquid Phase

Keiichi Ohno,[†] Takafumi Shimoaka,[†] Nobuyuki Akai,[‡] and Yukiteru Katsumoto*,[†]

Graduate School of Science, Hiroshima University, 1-3-1 Kagami-yama Higashi-Hiroshima 739-8526, Japan, Graduate school of science and engineering, Tokyo Institute of Technology, 2-12-1 Ookayama, Meguro, Tokyo 152-8551, Japan

Received: February 2, 2008; Revised Manuscript Received: May 18, 2008

The OH stretching (ν_{OH}) band of methanol observed in condensed phase has been analyzed in terms of hydrogen-bonding patterns. Quantum chemical calculations for methanol clusters have revealed that broadening of the ν_{OH} envelope is reasonably reproduced by considering nearest and next-nearest neighbor interactions through hydrogen bonding. Because the hydrogen bond formed between donor (D) and acceptor (A) is cooperatively strengthened or weakened by a newly formed hydrogen bond at D or A, we have proposed the following notation for hydrogen-bonding patterns of monohydric alcohols: a_DDA$d_A a_A$, where a is the number of protons accepted by D (a_D) or A (a_A), and d_A is the number of protons donated by A. The indicator of the hydrogen-bond strength, which is given by $M_{OH} = a_D + d_A - a_A$, is correlated well with the ν_{OH} wavenumber of the methanol molecule D participating in the a_DDA$d_A a_A$ pattern. The correlation between M_{OH} and the hydrogen-bonding energy of the a_DDA$d_A a_A$ pattern has also been deduced from the calculation results for the clusters. The ν_{OH} bands of methanol measured in the CCl_4 solution and pure liquid have been successfully analyzed by the method proposed here.

1. Introduction

Methanol is a highly structured liquid at ambient temperature, in which the molecules interact with each other through hydrogen bonding. The measurement of the OH stretching (ν_{OH}) band has proved to be a sensitive indicator of the strength of the hydrogen bond.[1–4] The ν_{OH} band shows a drastic change in its wavenumber and intensity depending upon the formation of hydrogen bond. The ν_{OH} envelope of methanol in condensed phase has a broad feature, which is generally attributed to the presence of various hydrogen-bonded aggregates. In this context, the ν_{OH} bands for methanol clusters have attracted keen interests.[5–16] The monomer, dimer, trimer, tetramer, and polymer $(CH_3OH)_n$ ($n > 4$) were identified by matrix-isolation infrared (IR) spectroscopy.[6–8] The small clusters with $n < 5$ were also found by IR spectroscopy in a pulsed supersonic slit-jet expansion system[14] and IR cavity ring-down spectroscopy.[15] However, the interpretation of the broad ν_{OH} envelope for methanol in the pure liquid and concentrated solutions is still the subject of much discussion because of its structureless feature. Several researchers pointed out that the ν_{OH} envelope of liquid methanol seems to be represented by one Gaussian function.[10] Because methanol molecules can form a percolated network through hydrogen bonding in condensed phase, the analytical model based on the limit size clusters may not be appropriate.

The broadening of the ν_{OH} envelope of methanol may arise not only from the presence of various aggregates but also from the cooperativity of hydrogen bonding.[17–19] The cooperativity plays an important role in the formation of hydrogen-bonded aggregates; the strength of a newly formed hydrogen bond is significantly influenced by the presence of already formed hydrogen bonds. Because the ν_{OH} wavenumber correlates with the strength of hydrogen bond, the cooperativity should significantly affect the feature of the ν_{OH} band of methanol. To link spectral information to microscopic information on hydrogen bonds, therefore, we must consider both the hydrogen-bonding patterns and the cooperativity. In this paper, we propose a novel method to analyze the broad ν_{OH} envelope of methanol observed in condensed phase. The purpose here is not to clarify what kind of methanol clusters exist in the solution and pure liquid but to interpret what kind of hydrogen-bonding patterns are dominant. First, we modify the notation of hydrogen-bonding patterns for investigating the ν_{OH} envelope of water,[20] in which the cooperativity of hydrogen bonding is estimated by considering the nearest and next-nearest neighbor interactions. For the methanol system, 12 hydrogen-bonding patterns can be distinguished. Second, we employ the quantum chemical calculation to link the ν_{OH} wavenumbers with the hydrogen-bonding patterns incorporated into the methanol clusters. As a result, the ν_{OH} wavenumbers of the 12 patterns can be categorized into five. This method enables us to investigate the change in the broad and structureless ν_{OH} envelope of methanol in condensed phase in terms of the variation in the hydrogen-bonding patterns.

2. Quantum Chemical Calculation

Quantum chemical calculations were performed by using the Gaussian 03 program.[21] Optimal geometries, harmonic wavenumbers, and IR intensities of methanol clusters $(CH_3OH)_n$ with $n = 1-7$ were obtained by the density functional theory (DFT) by using the 6-311++G(d,p) basis set.[17,22] For DFT calculations, we used Becke's three-parameter exchange functional together with correlation functional of Lee−Yang−Parr (B3LYP).[23,24] Harmonic wavenumbers ν_{harm} obtained by DFT calculations were scaled by the formula $\nu_{OH} = \nu_{harm}(1.2155 - 0.00007\nu_{harm})$.[25–27] The normal vibrations were calculated for two types of isotope

* To whom all correspondence should be sent. Fax: +81-82-424-7408. E--mail: katsumot@hiroshima-u.ac.jp.
† Hiroshima University.
‡ Tokyo Institute of Technology.

10.1021/jp800995m CCC: $40.75
Published on Web 07/18/2008

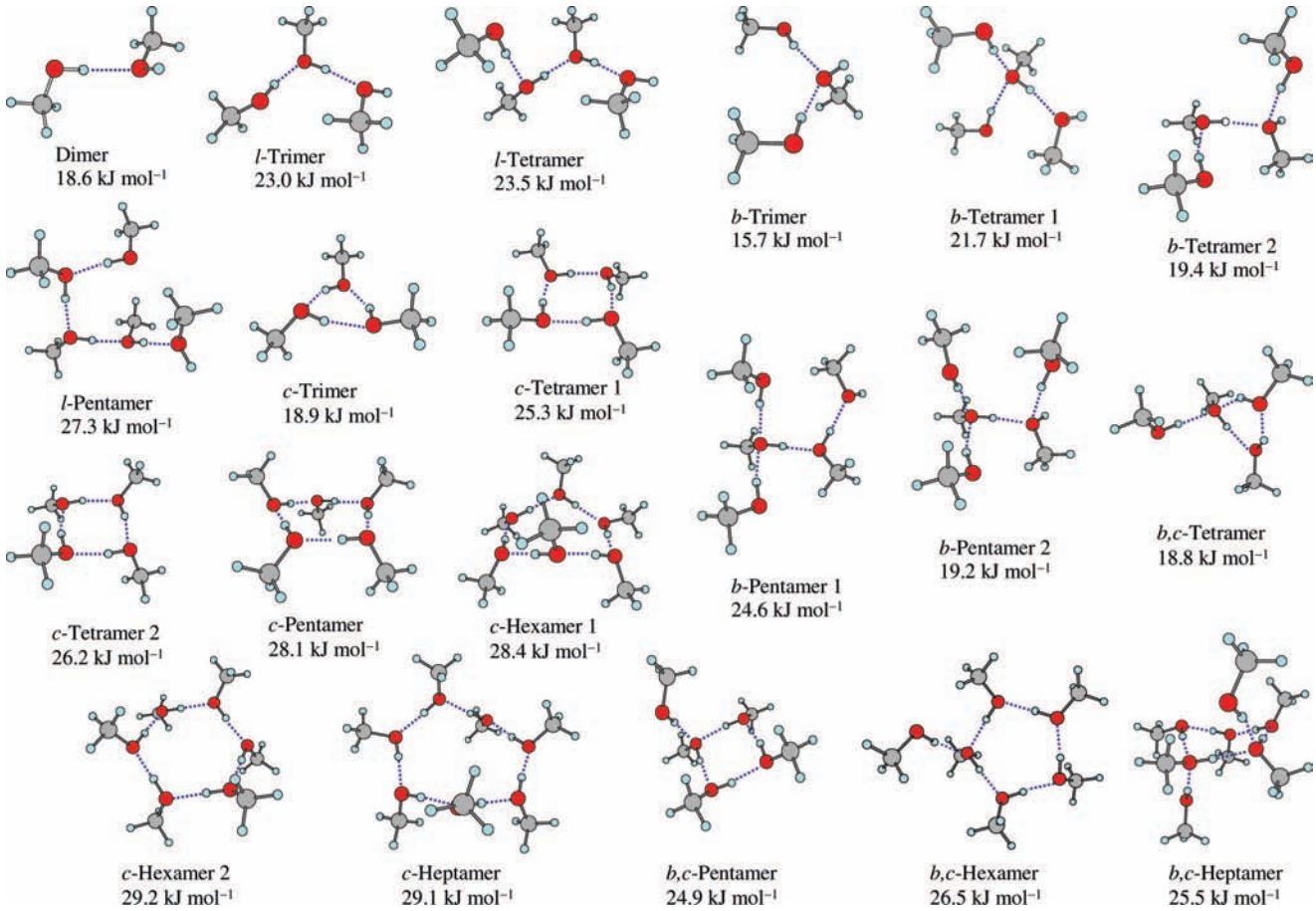

Figure 1. Geometries of methanol clusters $(CH_3OH)_n$ with $n = 2-7$ optimized at the B3LYP/6-311++G(d,p) level. The linear, cyclic, and branched structures are indicated by *l*-, *c*-, and *b*-, respectively. The average hydrogen-bonding energy for each structure, $\Delta\bar{E}_{hb}$, is indicated below the structure (see text for the definition). The dotted line represents the OH···O hydrogen bond.

clusters. The coupled ν_{OH} wavenumbers were calculated for methanol (CH_3OH) embedded in clusters constituted of CH_3OH molecules. The uncoupled ν_{OH} wavenumbers were calculated for CH_3OH surrounded by deuterated methanol (CH_3OD) molecules in the same clusters.[28,29] The total and average energy of hydrogen bonding, ΔE_{hb} and $\Delta\bar{E}_{hb}$, are defined by the following equations

$$\Delta E_{hb} = nE(\text{monomer}) - E(\text{n-mer}) \quad (1a)$$

$$\Delta\bar{E}_{hb} = \frac{\Delta E_{hb}}{m} \quad (1b)$$

where E(monomer) is the electronic energy for the monomer, E(*n*-mer) is the electronic energy for the *n*-mer, *n* is the number of methanol molecules participating in the cluster, and *m* is the number of hydrogen bonds in the cluster. The zero-point energy correction was carried out for E(monomer) and E(*n*-mer) of the undeuterated systems.

3. Experimental Section

The CH_3OD was obtained from Aldrich. The purity of the sample is ca. 98% (the isotopic purity is higher than 99%). The CH_3OH and carbon tetrachloride (CCl_4) were purchased from Wako (∞ pure grade, the purity is 99.8%). All chemicals were used without further purification. IR spectra were recorded on a Bruker IFS66V vacuum spectrophotometer equipped with a deuterated triglycine sulfate (DTGS) detector by coaddition of 256 scans at a resolution of 2 cm^{-1}. To measure the uncoupled ν_{OH} band, we prepared an isotope mixture that contained 1 wt% of CH_3OH in CH_3OD as the pure liquid of methanol. A CCl_4 solution of methanol with the isotope mixture was also prepared, in which the total methanol concentration was 0.10 mol dm^{-3}. We used the quartz cell with 10 mm of path length for the CCl_4 solution and the CaF_2 cell with 0.1 mm of path length for the pure liquid. The sample cells were placed in a homemade holder temperature-regulated by a Peltier device.

Nonlinear curve fittings and principal-component analysis (PCA) were performed by a software written by one of the authors (Y.K.).[30] The Levenberg−Marquardt algorithm[31] for a nonlinear least-squares method was used for the curve-fitting procedure. The position and number of the peaks used in the curve fitting were estimated by third derivative, and the shape of the decomposed band was assumed to be a linear combination of Gaussian and Lorentzian functions. Third derivatives were calculated by the Savitzky−Golay method.[32] PCA was performed by finding eigenvalues and eigenvectors of a tridiagonal matrix calculated from the experimental IR spectra.[33] The Householder method was used to obtain the tridiagonal form of data matrix. The QL algorithm with implicit shifts was employed to determine the eigenvalues and eigenvectors.[31]

4. Results and Discussion

4.1. Relationship between the ν_{OH} Wavenumbers and Hydrogen-Bonding Patterns for Methanol Clusters. Figure 1 shows the optimized geometries for methanol clusters, together with $\Delta\bar{E}_{hb}$. The coupled and uncoupled ν_{OH} wavenumbers of methanol clusters are given in Table 1. All the free OH-bond lengths are calculated to be 0.962 ± 0.02 Å (1 Å = 10^{-10} m).[34]

TABLE 1: Calculated ν_{OH} Wavenumbers of Methanol Clusters $(CH_3OH)_n$ with $n = 1$-7

coupled ν_{OH}/cm^{-1} (absorbance/km mol^{-1}) uncoupled ν_{OH}/cm^{-1}					assignment	
					a_DDA$d_A a_A$	M_{OH}
monomer	dimer	*l*-trimer	*l*-tetramer	*l*-pentamer		
3639 (31)	3639 (44) 3639	3644 (43) 3644	3645 (47) 3645	3643 (44) 3642	Free	
	3533 (508) 3533				0DA00	0
		3483 (683) 3475	3478 (600) 3476	3448 (646) 3449	1DA00	1
		3450 (583) 3460	3471 (621) 3467	3415 (682) 3408	0DA10	1
			3362 (959) 3369	3365 (1314) 3359	1DA10	2
				3309 (942) 3327	1DA10	2

b-trimer	*b*-tetramer 1	*b*-tetramer 2	*b*-pentamer 1	*b*-pentamer 2		
3626 (53) 3626	3641 (50) 3642	3631 (55) 3630	3643 (45) 3643	3631 (59) 3630	Free	
3558 (299) 3553		3565 (341) 3565		3585 (256) 3589	0DA01	−1
3547 (526) 3553					0DA01	−1
	3515 (378) 3507		3498 (449) 3493	3544 (447) 3538	0DA11	0
	3494 (702) 3500		3462 (1026) 3464	3517 (376) 3519	0DA11	0
		3505 (596) 3500			1DA01	0
		3469 (521) 3474			0DA10	1
			3451 (434) 3449		1DA00	1
				3446 (663) 3447	2DA01	1
	3392 (853) 3397				2DA00	2
			3247 (1219) 3255		2DA10	3

c-trimer	*c*-tetramer 1	*c*-tetramer 2	*c*-pentamer		
3478 (790) 3468	3395 (0) 3368	3384 (174) 3350	3367 (141) 3341	1DA10	2
3471 (832) 3460	3394 (1807) 3368	3357 (1847) 3350	3357 (396) 3331	1DA10	2
3433 (27) 3453	3365 (1951) 3361	3357 (1855) 3350	3326 (2391) 3322	1DA10	2
	3308 (0) 3361	3292 (1) 3351	3318 (2516) 3320	1DA10	2
			3261 (57) 3319	1DA10	2

c-hexamer 1	*c*-hexamer 2	*c*-heptamer		
3367 (136) 3340	3354 (749) 3313	3367 (324) 3342	1DA10	2
3358 (524) 3339	3339 (0) 3312	3362 (846) 3328	1DA10	2
3350 (467) 3325	3338 (0) 3312	3346 (91) 3324	1DA10	2
3314 (2725) 3322	3296 (3156) 3312	3339 (108) 3324	1DA10	2
3307 (2902) 3321	3295 (3151) 3311	3303 (3258) 3323	1DA10	2
3260 (24) 3319	3241 (0) 3312	3300 (3461) 3322	1DA10	2
		3258 (25) 3320	1DA10	2

b,c-tetramer	*b,c*-pentamer	*b,c*-hexamer	*b,c*-heptamer		
3521 (423) 3513	3507 (472) 3502	3502 (542) 3498	3505 (630) 3503	0DA11	0
			3498 (433) 3493	0DA11	0
3505 (630) 3510	3460 (635) 3461	3431 (579) 3430	3444 (496) 3443	1DA11	1
3481 (474) 3481	3360 (1248) 3348	3358 (551) 3333	3349 (1385) 3353	1DA10	2
	3320 (779) 3320	3323 (1936) 3335	3260 (828) 3251	1DA10	2
		3292 (1420) 3296		1DA10	2
			3361 (1120) 3359	2DA11	2
3357 (691) 3370	3250 (996) 3273	3216 (960) 3240	3174 (1265) 3201	2DA10	3

The OH-bond length (r_{OH}) of the hydrogen donor in cyclic clusters is elongated from 0.974 to 0.986 Å with increasing n from 3 to 6. For the same size cluster, ΔE_{hb} falls in the following order: cyclic > branched cyclic > linear chain > branched chain. It is worth noting that the number of hydrogen bonds in the cyclic structure is always greater by one than that in the same size cluster with the chain. As seen in Figure 1, the $\Delta\bar{E}_{hb}$ value calculated for methanol clusters does not exceed 30 kJ mol^{-1}. The $\Delta\bar{E}_{hb}$ of 25−30 kJ mol^{-1} is very close to the largest value of hydrogen bonding for several monohydric alcohols in condensed phase estimated by quantum chemical calculations,[17,35] Monte Carlo simulation study,[36] and by Raman and IR spectroscopy.[37] This value also corresponds to the average hydrogen-bond energy of monohydric alcohols in the pure liquid deduced by thermodynamic consideration.[38] Several researchers pointed out that the average hydrogen-bond energy of monohydric alcohols reaches a limiting value of ca. 30 kJ mol^{-1} even if the size of clusters keeps increasing in the system.[37] It is therefore likely that the upper limit value of the cooperative hydrogen-bond energy for methanol is around 30 kJ mol^{-1}.

To link the ν_{OH} wavenumber with the hydrogen-bonding pattern of monohydric alcohols, we expand the notation used for the hydrogen-bonding pattern of water.[20] First, the OH···O hydrogen bond between donor (D) and acceptor (A) alcohols is denoted as DA. When another alcohol molecule newly participates into the DA hydrogen bond, the bond strength is changed (the so-called cooperativity of hydrogen bonding). Both D and A are capable of forming hydrogen bonds with the other methanol molecules; D can accept two protons, whereas A can donate and/or accept one proton. To consider the cooperativity of hydrogen bonding, the hydrogen-bonding pattern of monohydric alcohols is represented as a_DDA$d_A a_A$, where a is the number of protons accepted by D (a_D) or A (a_A), and d_A is the number of protons donated by A. The d_A and a_A vary from 0 to 1, and a_D ranges from 0 to 2. In this method, therefore, the cooperative of hydrogen bonding is estimated by considering

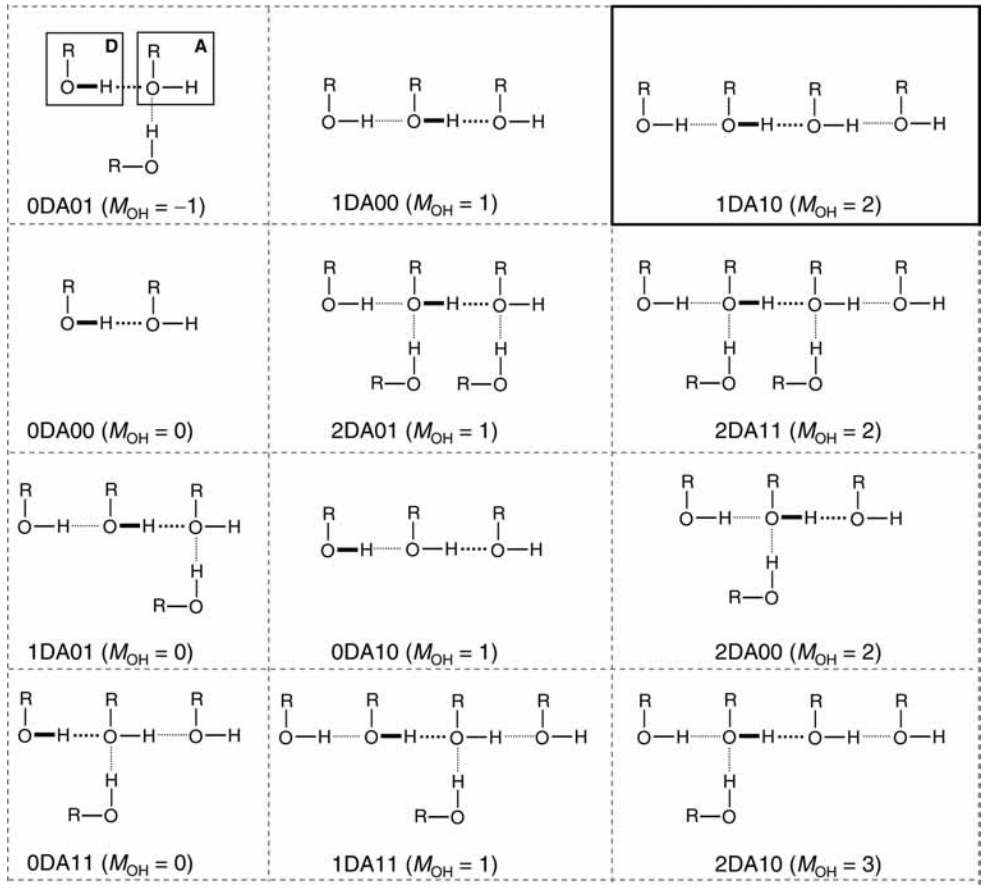

Figure 2. Schematic images of possible hydrogen-bonding patterns a_DDA$d_A a_A$ for monohydric alcohol clusters (see text for details). The M_{OH} value is also given for each pattern. The two-coordinate methanol chain is indicated in the square with solid line.

the interactions of nearest and next-nearest neighbors. The hydrogen-bonding patterns found in the methanol clusters are listed in Table 1, together with their ν_{OH} wavenumbers.

The DA strength changes depending upon the hydrogen-bonding pattern a_DDA$d_A a_A$. To classify the hydrogen-bond strength of methanol, we introduce the indicator $M_{OH} = a_D + d_A - a_A$. The DA is strengthened with increasing a_D and/or d_A but weakened with increasing a_A. As a result, the M_{OH} value ranges from −1 to 3. Figure 2 shows schematic images for the relationship between M_{OH} and the possible hydrogen-bonding patterns of monohydric alcohols. When DA is isolated, the hydrogen-bonding pattern is represented by 0DA00 with $M_{OH} = 0$. A positive value of M_{OH} indicates that the DA strength increases compared with that for the pattern with $M_{OH} = 0$. In the case where M_{OH} is negative, the DA strength decreases. It is worth reminding that the 1DA01 and 0DA11 patterns also give $M_{OH} = 0$. By using the M_{OH} value, one can predict that the 2DA10 pattern with $M_{OH} = 3$ causes the most strengthened DA. The ν_{OH} band due to the methanol molecule that is not the proton donor appears at the highest wavenumber region. These bands are represented as Free in this paper.

In Figure 3, the uncoupled and coupled ν_{OH} wavenumbers are plotted as a function of r_{OH}. Figure 3A reveals a linear relationship between the uncoupled ν_{OH} wavenumber and r_{OH}. A similar tendency was previously reported.[39,40] As shown in Figure 3A, the ν_{OH} wavenumbers of the hydrogen-bonding patterns with the same M_{OH} are close to each other. In other words, the ν_{OH} wavenumber region of methanol is separated into six regions characterized by M_{OH}, although there is overlap. The width of the wavenumber region for each M_{OH} reflects the variety of the hydrogen-bonding geometries of the a_DDA$d_A a_A$ patterns. When the hydrogen bond is formed under constrained geometries, the ν_{OH} wavenumber appears far from a moderate

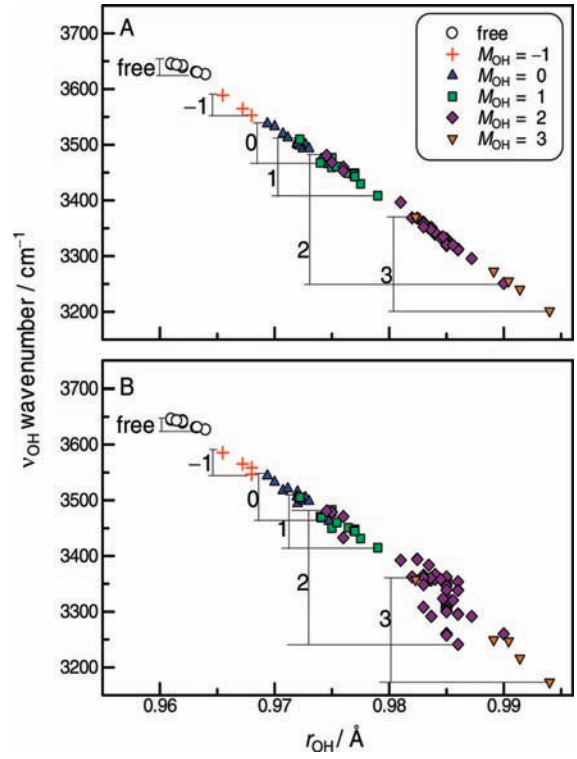

Figure 3. Relationship between the ν_{OH} wavenumbers and r_{OH} calculated for methanol clusters $(CH_3OH)_n$ with $n = 1-7$ in the uncoupled (A) and coupled (B) systems.

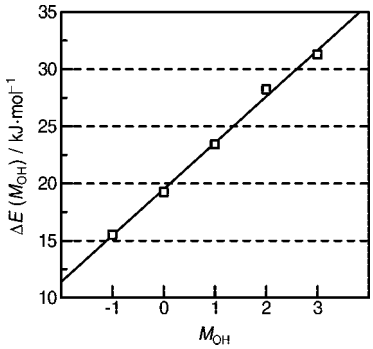

Figure 4. The hydrogen-bonding energy of the hydrogen-bonding pattern with M_{OH}, $\Delta E(M_{OH})$, plotted against the M_{OH} index.

position. For example, the ν_{OH} wavenumbers (ca. 3470 cm^{-1}) for the cyclic trimer are much higher than those (3360–3320 cm^{-1}) for the cyclic tetramer, pentamer, and hexamer because of the strained O−H···O angle (see Table 1 and Table S1 in the Supporting Information),[34] even if all of the hydrogen-bonding patterns are 1DA10 ($M_{OH} = 2$) in the cyclic cluster. In Figure 3B, we found that several points are deviated from the linear correlation line, especially in the wavenumber region of $M_{OH} = 2$. The deviation may be caused by the coupling among the OH stretching modes.[28,29] By comparing panels A and B of Figure 3, we can conclude that the ν_{OH} wavenumber due to the a_DDA$d_A a_A$ pattern can be characterized by M_{OH} for both uncoupled and coupled systems, although the vibrational coupling changes the width of the wavenumber region.

It is very interesting to establish the correlation between M_{OH} and the hydrogen-bond energy of the a_DDA$d_A a_A$ patterns. Because this kind of information cannot be directly extracted from the calculation results, we employed the multiple linear regression (MLR) analysis[31] on ΔE_{hb} by assuming following equation:

$$\Delta E_{hb} = \sum_{M_{OH}=-1}^{3} n_{M_{OH}} \Delta E(M_{OH}) \qquad (2)$$

where $n_{M_{OH}}$ is the number of the hydrogen-bonding patterns with M_{OH} involved in one cluster and $\Delta E(M_{OH})$ is the hydrogen-bonding energy allocated to each M_{OH} value. In the eq 2, it is assumed that ΔE_{hb} of each cluster is equal to the sum of the energies of the hydrogen-bonding patterns with M_{OH} involved in the cluster. The MLR analysis was carried out to determine the five variables of $\Delta E(M_{OH})$ ($-1 < M_{OH} < 3$) by using the calculation results for the methanol clusters illustrated in Figure 1. Note that the data for *c*-trimer and *b,c*-tetramer is not used in the MLR analysis, because their hydrogen bonds are formed under significant constrained conditions. Figure 4 shows the result of the MLR analysis, and a linear correlation between $\Delta E(M_{OH})$ and M_{OH} was found. Thus, we concluded that the M_{OH} index corresponds to the hydrogen-bond strength of DA.

4.2. Temperature Dependence of the ν_{OH} Envelope of Methanol in a CCl_4 Solution. The uncoupled and coupled ν_{OH} bands of methanol in CCl_4 at a concentration of 0.10 mol dm^{-3} were measured with varying temperature from 283 to 333 K with increments of 5 K. Figure 5 depicts the uncoupled ν_{OH} envelope of methanol in the CCl_4 solution at 298, 308, and 328 K, together with the curve-fitting and PCA results. Figure 6 shows the temperature dependence of the coupled ν_{OH} envelope. The first PCA eigenvector represents the invariant component through the entire temperature region. The second and third PCA eigenvectors suggest that the ν_{OH} envelope of methanol contains

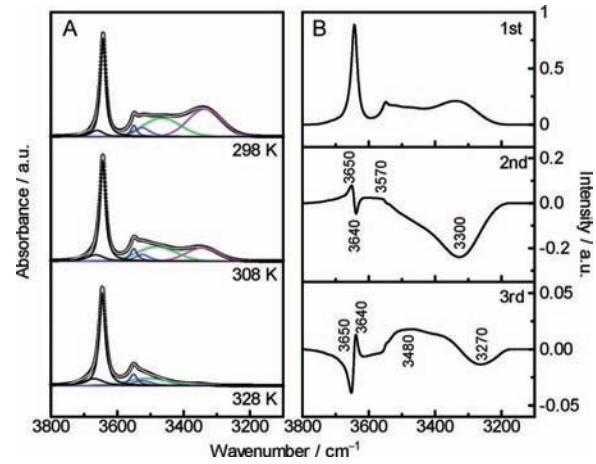

Figure 5. (A) Uncoupled ν_{OH} envelopes of methanol measured in the 0.10 mol dm^{-3} CCl_4 solution at 298, 308, and 328 K and their curve fitting results. (B) PCA results for the temperature dependence of the IR spectra of methanol in CCl_4.

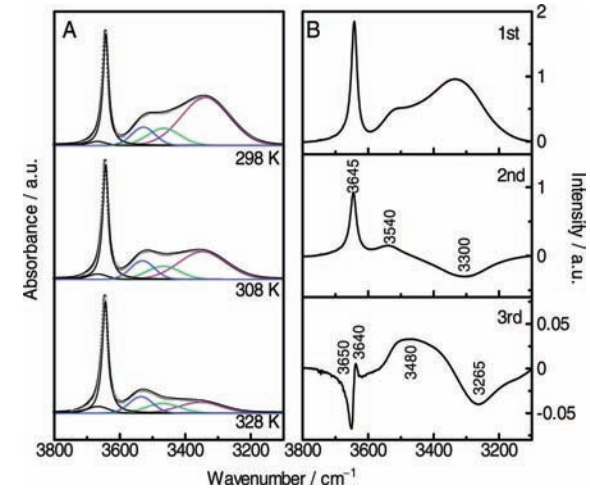

Figure 6. (A) Coupled ν_{OH} envelope of methanol measured in the 0.10 mol dm^{-3} CCl_4 solution at 298, 308, and 328 K and their curve fitting results. (B) PCA results for the temperature dependence of the IR spectra of methanol in CCl_4.

several independent bands, which change their relative intensities with rising temperature. By comparing Figure 5 with Figure 6, one can remark that the overlap of the coupled ν_{OH} bands is more severe than that of the uncoupled bands. According to PCA and third-derivative calculations, the uncoupled and coupled ν_{OH} envelopes were reasonably decomposed into six and five components by curve fitting, respectively. The marked difference between uncoupled and couple ν_{OH} envelopes is found in the 3600−3400 cm^{-1} region; three bands around 3550, 3525, and 3475 cm^{-1} were identified for the uncoupled system, whereas two bands around 3540 and 3470 cm^{-1} were obtained for the coupled one. The uncoupled ν_{OH} band at 3550 cm^{-1} may arise from the methanol dimer, which cannot be identified under the coupled condition.

According to Figure 3, the uncoupled and coupled ν_{OH} bands observed for methanol in CCl_4 can be associated with M_{OH}; Free (3670−3640 cm^{-1}), $M_{OH} = 0$ (3550−3520 cm^{-1}), $M_{OH} = 1$ (3520−3440 cm^{-1}), and $M_{OH} = 2$ (3360−3320 cm^{-1}). Figure 7 shows the changes in the relative intensity of the ν_{OH} bands decomposed by the curve fitting. For both the uncoupled and coupled systems, a similar tendency was obtained. It should be noted that the relationship between the relative IR intensity and the population functions of the hydrogen-bonding patterns

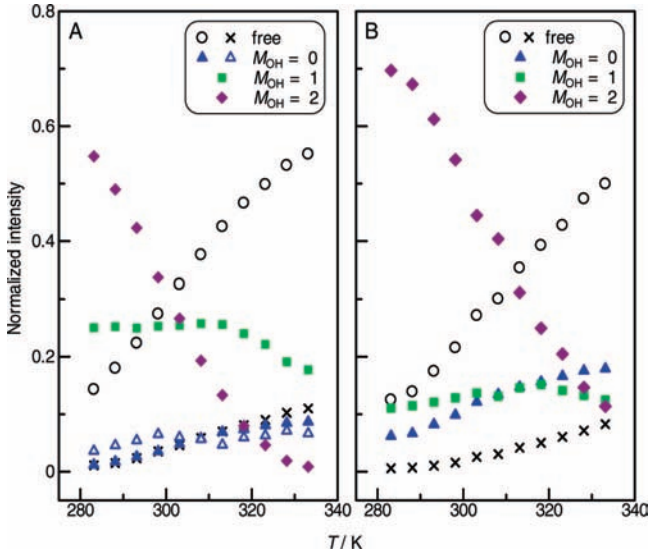

Figure 7. Temperature dependence of the normalized integral intensities for the uncoupled (A) and coupled (B) ν_{OH} bands of methanol in the 0.10 mol dm^{-3} CCl_4 solution estimated by curve fitting.

is not straightforward because of the dependence of the IR intensities on the hydrogen bond (see also Table 1). The relative intensity of the band due to $M_{OH} = 2$ decreases with increasing temperature, whereas the bands due to Free and $M_{OH} = 0$ increase. The result may be related to the recombination of the patterns 1DA10 (2), 2DA11 (2), 2DA00 (2), 0DA00 (0), 1DA01 (0), and 0DA11 (0). The numbers in parentheses corresponds to the M_{OH} index. Several research groups have shown by simulation that methanol molecules in condensed phase prefer to form the hydrogen bond with the two-coordinate chain structures (1DA10) rather than the branched ones (2DA11 or 2DA00).[41–44] In a dilute CCl_4 solution, the linear chain and cyclic clusters may also exist.[38,45] The linear chain structures consist of the 1DA00(1), 0DA10 (1), and 1DA10 (2) patterns, whereas the cyclic clusters exclusively contain the 1DA10 (2) pattern. For methanol in the CCl_4 solution, therefore, the following interpretation is also possible: the changes in relative intensity of the ν_{OH} bands are attributed to the thermal dissociation of the linear chain and cyclic structures.

4.3. Temperature Dependence of the ν_{OH} Envelope of Methanol in the Pure Liquid. Figure 8 shows the uncoupled ν_{OH} envelope for the pure methanol liquid at 298, 308, and 328 K and the PCA result. The second and third PCA eigenvectors suggest the existence of the bands around 3510, 3470, 3370, 3300, and 3280 cm^{-1}. Therefore, the ν_{OH} envelope for the pure methanol liquid was decomposed into four bands at 3540, 3460, 3340, and 3250 cm^{-1} as shown in Figure 8A. It should be emphasized that no Free ν_{OH} band of methanol was observed for the pure liquid. The band at 3540 cm^{-1} is assignable to $M_{OH} = 0$. Because the ν_{OH} band due to Free is not observed, the $M_{OH} = 0$ band should be directly associated with the 0DA11 pattern.[46] The 0DA11 pattern is related to the existence of an end-donor methanol molecule in the pure liquid. The band at 3460 cm^{-1} is assigned to $M_{OH} = 1$, which is associated with the 0DA10 and 1DA11 patterns. The 1DA00 (1) and 2DA01 (1) can be neglected, because no Free band is observed. The band at 3340 cm^{-1} is due to $M_{OH} = 2$, which arises from the 1DA10 and 2DA11 patterns (2DA00 can be ignored). The two-coordinate network, which has often been reported for the hydrogen bonding of methanol in the pure liquid,[41–44] is represented by 1DA10 (2). The band at 3250 cm^{-1} is linked to $M_{OH} = 3$, which is related to the 2DA10 pattern. The bands at

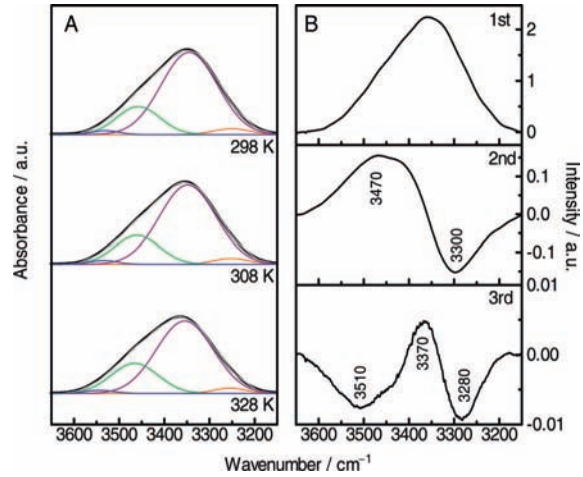

Figure 8. (A) Uncoupled ν_{OH} envelopes of methanol measured in the pure liquid at 298, 308, and 328 K and their curve fitting results. (B) PCA results for the temperature dependence of IR spectra of the pure liquid methanol.

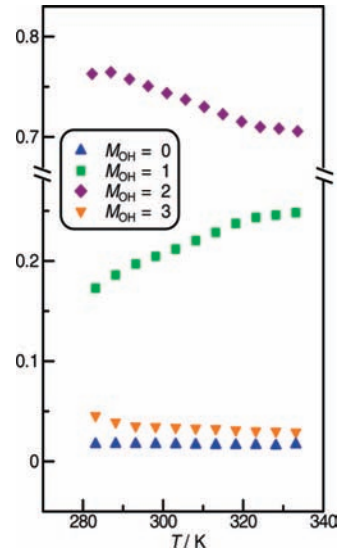

Figure 9. Temperature dependence of the normalized integral intensities for the uncoupled ν_{OH} bands of methanol in the pure liquid estimated by curve fitting.

3540 (0) and 3250 (3) cm^{-1} may arise from the branched networks of methanol in the pure liquid.

Figure 9 represents the thermal changes in the relative intensity of the bands due to $M_{OH} = 0$, 1, 2, and 3. The $M_{OH} = 2$ band is dominant throughout the entire temperature range investigated. The relative intensity of the $M_{OH} = 1$ band increases as the temperature goes up, whereas the $M_{OH} = 2$ band decreases in relative intensity. On the other hand, the temperature dependences of the $M_{OH} = 0$ and 3 bands are very small. Because M_{OH} is correlated with the hydrogen-bond strength as shown in Figure 4, the spectral change reflects that the hydrogen-bonding patterns of methanol shift from strengthened patterns to weakened ones as the temperature rises. In the case where methanol molecules prefer to form the two-coordinate network in condensed phase as reported previously,[41–44] the thermal changes in the IR spectra of the pure methanol liquid may arise from the thermal dissociation of the two-coordinate network and the increase in the branched chain structures.

5. Conclusion

In the present paper, we proposed a method for analyzing the broad ν_{OH} band of methanol in condensed phase. Because

methanol molecules can form a percolated network through hydrogen bonding in condensed phase, the analytical model based on the limit size clusters may not be appropriate. The spectral simulation of methanol clusters revealed that the ν_{OH} wavenumbers are reasonably approximated by considering nearest and next-nearest neighbor interactions. The strength of the OH···O hydrogen bond between D and A, which is denoted as DA, is cooperatively increased or decreased by a newly formed hydrogen bond at D and/or A. To consider the cooperativity of hydrogen bond, we represented the hydrogen-bonding pattern as $a_D DA d_A a_A$, where a is the number of protons accepted by D (a_D) or A (a_A), and d_A is the number of protons donated by A. The M_{OH} index, which is defined as $M_{OH} = a_D + d_A - a_A$, reflects the DA strength and the ν_{OH} wavenumber of D. As a result, the ν_{OH} wavenumber region of methanol is classified into six regions (Free and $M_{OH} = -1$, 0, 1, 2, and 3). The ν_{OH} band due to the methanol that is not the proton donor is represented as Free.

The ν_{OH} envelope of methanol in the CCl_4 solution and pure liquid was successfully analyzed by using the $a_D DA d_A a_A$ patterns and M_{OH}. The temperature dependence of the ν_{OH} band for methanol in CCl_4 indicated that the relative intensity of the band due to $M_{OH} = 2$ decreases with increasing temperature, whereas the bands due to Free and $M_{OH} = 0$ increase. The result is related to the recombination of the patterns 1DA10 (2), 2DA11 (2), 2DA00 (2), 0DA00 (0), 1DA01 (0), and 0DA11 (0). For the pure liquid of methanol, the band due to $M_{OH} = 2$ (1DA10 and 2DA11 patterns) is dominant throughout the entire temperature range investigated. The relative intensity of the $M_{OH} = 1$ (0DA10 and 1DA11 patterns) band increases as the temperature goes up, whereas that of the $M_{OH} = 2$ band decreases. On the other hand, the temperature dependence of the $M_{OH} = 0$ (0DA11 pattern) and 3 (2DA10 pattern) bands are very small. Because M_{OH} is correlated with the hydrogen-bond strength, the spectral change reflects that the hydrogen-bonding patterns of methanol shift from strengthened patterns to weakened ones as the temperature rises.

Acknowledgment. This work was partially supported by a Grant-in-Aid for Scientific Research no. 16205003 from the Ministry of Education, Culture, Sports, Science, and Technology (MEXT) of the Japanese Government.

Supporting Information Available: Structural parameters of optimized structures for methanol clusters. This material is available free of charge via the Internet at http://pubs.acs.org.

References and Notes

(1) Glew, D. N.; Rath, N. S. *Can. J. Chem.* **1971**, *49*, 837.
(2) Van Ness, H. C.; Van Winkle, J.; Richtol, H. H.; Hollinger, H. B. *J. Phys. Chem.* **1967**, *71*, 1483.
(3) Dixon, J. R.; George, W. O.; Hossain, Md.F.; Lewis, R.; Price, J. M. *J. Chem. Soc. Faraday Trans.* **1997**, *93*, 3611.
(4) Pimentel, G. C.; McClellan, A. L. *The Hydrogen Bond*; W.H. Freeman and Co.: San Francisco, 1960; pp 67−141.
(5) Buck, U.; Huisken, F. *Chem. Rev.* **2000**, *100*, 3863.
(6) Van Thiel, M.; Becker, E. D.; Pimentel, G. C. *J. Chem. Phys.* **1957**, *27*, 95.
(7) Han, S. W.; Kim, K. *J. Phys. Chem.* **1996**, *100*, 17124.
(8) Perchard, J. P.; Mielke, Z. *Chem. Phys.* **2001**, *264*, 221.
(9) Coussan, S.; Loutellier, A.; Perchard, J. P.; Racine, S.; Peremans, A.; Tadjeddine, A.; Zheng, W. Q. *J. Chem. Phys.* **1997**, *107*, 6526.
(10) Kristiansson, O. *J. Mol. Struct.* **1999**, *477*, 105.
(11) Huisken, F.; Kulcke, A.; Laush, C.; Lisy, J. M. *J. Chem. Phys.* **1991**, *95*, 3924.
(12) Huisken, F.; Kaloudis, M.; Koch, M.; Werhahn, O. *J. Chem. Phys.* **1996**, *105*, 8965.
(13) Buck, U.; Ettischer, I. *J. Chem. Phys.* **1998**, *108*, 33.
(14) Häber, T.; Schmitt, U.; Suhm, M. A. *Phys. Chem. Chem. Phys.* **1999**, *1*, 5573.
(15) Provencal, R. A.; Paul, J. B.; Roth, K.; Chapo, C.; Casaes, R. N.; Saykally, R. J.; Tschumper, G. S.; Schaefer, H. F., III *J. Chem. Phys.* **1999**, *110*, 4258.
(16) Pribble, R. N.; Hagemeister, F. C.; Zwier, T. S. *J. Chem. Phys.* **1997**, *106*, 2145.
(17) Hagemeister, F. C.; Gruenloh, C. J.; Zwier, T. S. *J. Phys. Chem. A* **1998**, *102*, 82.
(18) Luck, W. A. P. *J. Mol. Struct.* **1998**, *448*, 131.
(19) Akiyama, M.; Torii, H. *Spectrochim. Acta.* **2000**, *A56*, 137.
(20) Ohno, K.; Okimura, M.; Akai, N.; Katsumoto, Y. *Phys. Chem. Chem. Phys.* **2005**, *7*, 3005.
(21) Frisch, M. J.; Trucks, G. W.; Schlegel, H. B.; Scuseria, G. E.; Robb, M. A.; Cheeseman, J. R.; Montgomery, J. A., Jr.; Vreven, T.; Kudin, K. N.; Burant, J. C.; Millam, J. M.; Iyengar, S. S.; Tomasi, J.; Barone, V.; Mennucci, B.; Cossi, M.; Scalmani, G.; Rega, N.; Petersson, G. A.; Nakatsuji, H.; Hada, M.; Ehara, M.; Toyota, K.; Fukuda, R.; Hasegawa, J.; Ishida, M.; Nakajima, T.; Honda, Y.; Kitao, O.; Nakai, H.; Klene, M.; Li, X.; Knox, J. E.; Hratchian, H. P.; Cross, J. B.; Bakken, V.; Adamo, C.; Jaramillo, J.; Gomperts, R.; Stratmann, R. E.; Yazyev, O.; Austin, A. J.; Cammi, R.; Pomelli, C.; Ochterski, J. W.; Ayala, P. Y.; Morokuma, K.; Voth, G. A.; Salvador, P.; Dannenberg, J. J.; Zakrzewski, V. G.; Dapprich, S.; Daniels, A. D.; Strain, M. C.; Farkas, O.; Malick, D. K.; Rabuck, A. D.; Raghavachari, K.; Foresman, J. B.; Ortiz, J. V.; Cui, Q.; Baboul, A. G.; Clifford, S.; Cioslowski, J.; Stefanov, B. B.; Liu, G.; Liashenko, A.; Piskorz, P.; Komaromi, I.; Martin, R. L.; Fox, D. J.; Keith, T.; Al-Laham, M. A.; Peng, C. Y.; Nanayakkara, A.; Challacombe, M.; Gill, P. M. W.; Johnson, B.; Chen, W.; Wong, M. W.; Gonzalez, C.; Pople, J. A. *Gaussian 03*; Gaussian, Inc.: Wallingford, CT, 2004.
(22) El Firdoussi, A.; Esseffar, M.; Bouab, W.; Abboud, J.-L. M.; Mó, O.; Yáñez, M.; Ruasse, M. F. *J. Phys. Chem. A* **2005**, *109*, 9141.
(23) Becke, A. D. *J. Chem. Phys.* **1993**, *98*, 5648.
(24) Lee, C.; Yang, W.; Parr, G. R. *Phys. Rev. B* **1988**, *37*, 785.
(25) Yoshida, H.; Ehara, A.; Matsuura, H. *Chem. Phys. Lett.* **2000**, *325*, 477.
(26) Matsuura, H.; Yoshida, H. In *Handbook of Vibrational Spectroscopy*; Chalmers, J. M. , Griffiths, P. R. , Eds; John Wiley & Sons Inc.: New York, 2001; Vol *3*, p S4203.
(27) Yoshida, H.; Takeda, K.; Okamura, J.; Ehara, A.; Matsuura, H. *J. Phys. Chem.* **2002**, *106*, 3580.
(28) Hermansson, K.; Ojamäe, L. *Intern. J. Quantum Chem.* **1992**, *42*, 1251.
(29) Hermansson, K.; Lidgren, J.; Probst, M. M. *Chem. Phys. Lett.* **1995**, *233*, 371.
(30) The software, named SPINA, can be downloaded from the following website: http://home.hiroshima-u.ac.jp/katsumot/spina.html
(31) Press, W. H.; Flannery, B. P.; Teukolsky, S. A.; Vetterling, W. T. *Numerical Recipes in C*; Cambridge University Press: Cambridge, U.K., 1988.
(32) Savitzky, A.; Golay, M. J. E. *Anal. Chem.* **1964**, *36*, 1627.
(33) Ozaki, Y.; Katsumoto, Y.; Jiang, J-H.; Liang, Y. In *Spectral analysis in the NIR region in Useful and Advanced Information in the Field of Near Infrared Spectroscopy*; Tsuchikawa, S. , Ed.; Research Signpost: Trivandrum India, 2003.
(34) Structural parameters of optimized structures for methanol clusters are listed in Table S1 of the Supporting Information.
(35) Sum, A. K.; Sandler, S. I. *J. Phys. Chem. A* **2000**, *104*, 1121.
(36) Stubbs, J. M.; Siepmann, J. I. *J. Phys. Chem. B* **2002**, *106*, 3968.
(37) Palombo, F.; Sassi, P.; Paolantoni, M.; Morresi, A.; Cataliotti, R. S. *J. Phys. Chem. B* **2006**, *110*, 18017.
(38) Benson, S. W. *J. Am. Chem. Soc.* **1996**, *118*, 10645.
(39) Kurita, E.; Matsuura, H.; Ohno, K. *Spectrochim. Acta* **2004**, *A60*, 3013.
(40) Badger, R. M. *J. Chem. Phys.* **1934**, *2*, 128.
(41) Jorgensen, W. L. *J. Am. Chem. Soc.* **1981**, *103*, 341.
(42) Matsumoto, M.; Gubbins, K. E. *J. Chem. Phys.* **1990**, *93*, 1981.
(43) Kosztolányi, T.; Bakó, I.; Pálinkás, G. *J. Chem. Phys.* **2003**, *118*, 4546.
(44) Pagliai, M.; Cardini, G.; Righini, R.; Schettino, U. *J. Chem. Phys.* **2003**, *119*, 6655.
(45) Sarker, S.; Joarder, R. N. *J. Chem. Phys.* **1993**, *99*, 2032.
(46) The 0DA00 and 1DA01 patterns should coexist with the Free band. See also Figure 2.

JP800995M